

RSC Advances



This is an *Accepted Manuscript*, which has been through the Royal Society of Chemistry peer review process and has been accepted for publication.

Accepted Manuscripts are published online shortly after acceptance, before technical editing, formatting and proof reading. Using this free service, authors can make their results available to the community, in citable form, before we publish the edited article. This *Accepted Manuscript* will be replaced by the edited, formatted and paginated article as soon as this is available.

You can find more information about *Accepted Manuscripts* in the [Information for Authors](#).

Please note that technical editing may introduce minor changes to the text and/or graphics, which may alter content. The journal's standard [Terms & Conditions](#) and the [Ethical guidelines](#) still apply. In no event shall the Royal Society of Chemistry be held responsible for any errors or omissions in this *Accepted Manuscript* or any consequences arising from the use of any information it contains.

ARTICLE

A facile approach to prepare biomimetic composite separators toward safety-enhanced lithium secondary batteries

Cite this: DOI: 10.1039/x0xx00000x

Taejoo Lee,^a Yunju Lee,^a Myung-Hyun Ryou,^{†a} and Yong Min Lee^{†a}

Received 00th January 2012,
Accepted 00th January 2012

DOI: 10.1039/x0xx00000x

www.rsc.org/

A mussel-inspired polydopamine (PDA) coating makes the radio-frequency (RF) Al₂O₃ sputtering a damage-free, reliable, and cost-efficient process, which thus far was not appropriate for the surface treatment of porous polyolefin-based separators. Due to thermally resistive PDA layers, polyethylene (PE) separators can sustain high-power Al₂O₃ sputtering conditions over 75 W, which significantly reduces processing time. Furthermore, compared to as-prepared separators, PDA/Al₂O₃-coated PE separators reveal improved thermal stability and cycle performances for lithium secondary batteries as well. PDA/Al₂O₃-coated PE separators held their original size when exposed to temperatures of 145°C during 30 min., while the bare PE separators shrank up to 9 % of the original size. At 25 °C temperature, the unit cell (LiMn₂O₄/separator/Li metal) employing the PDA/Al₂O₃-coated PE separators maintains 94.8 % (103.4 mAh g⁻¹) of the initial discharge capacity after 500 cycles at C/2 rate and 51.7 % (56.7 mAh g⁻¹) at 25 C rate, while corresponding values for the bare PE separators are 89 % (98.6 mAh g⁻¹) at C/2 rate and 24.5 % (27.2 mAh g⁻¹) at 25C rate, respectively.

Introduction

Due to high specific-energy density and long cycle life, lithium ion batteries (LIBs) are vital power sources predominantly used in consumer electronics.¹⁻⁵ With the ever-increasing demands for high energy density LIBs in emerging fields such as electric vehicles (EVs) and energy storage systems (ESSs), it has become imperative that a way be found to increase energy density of LIBs at lower cost.^{6,7} Especially for the large-scale applications of LIBs, the safety issue takes a pivotal position because consumer safety is a major concern for battery manufacturers. Fast charging accompanying high current and/or over-charging can cause lithium dendrite growth on the anode surface owing to the Li-insertion potential of conventional carbonaceous anodes which almost approaches to 0V vs. Li/Li⁺.⁸⁻¹¹ Out of the various battery constituents including anodes, cathodes, and electrolytes, the separators is the key to determining the safety of whole LIB system.^{5-7,12} As separators physically block a direct contact between cathodes and anodes, if the heat generated from large-scale batteries equipped with high-power energy devices rupture the dimensional stability of separators, a catastrophic thermal failure of LIBs would occur, accompanied by explosive flame and venting. To overcome these drawbacks, a large number of approaches have been undertaken to apply a surface coating on the commercial porous polyolefin-based (in particular, polyethylene (PE) and polypropylene (PP)) separators.¹³⁻¹⁶ Heat-resistant coating, including ceramic particles and/or high-melting polymers can effectively improve the thermal stability of the commercial polyolefin-based separators. On the other hand, the coating layers inherently alter the pore structure of the separators, and thus

influence the ionic pathway within the separators, which in turn affects the cell performances of the LIBs. In general, the coating layers upon separators likely to block and/or hinder the existing pore structure of separators.

To the best of our knowledge, we were the first to report the feasibility of using radio-frequency (RF) magnetron sputtering to introduce binder-free inorganic coating layers (Al₂O₃ in the study) onto commercial PE separators.¹⁷ An optimal amount of hydrophilic Al₂O₃ layers create desirable ionic pathways resulting in enhanced rate capabilities of LIBs without blocking the pores, which are beneficial to holding larger amount of liquid electrolytes. However, the sputtering time of longer than 10 minutes should be shortened to a few minutes for commercial application. Hence, in order to maintain the proper amount of sputtered coating materials, the RF power has to be increased, which might cause thermal damage to PE separators. A facile approach to circumvent this problem is pre-coat the bare separator with polydopamine (PDA) for enhancing thermal stability, followed by high-power RF sputtering.

Experimental

Materials

The cathode was prepared by mixing LiMn₂O₄ (LMO, Kyushu Ceramics, Japan), polyvinylidene fluoride (PVDF; KF-1300, Kureha, Japan), and conductive carbon (Super-P, Timcal, Switzerland). The anode was Li metal foil (400 μm, Honjo Metal, Japan). A mixture of ethylene carbonate/ethyl methyl carbonate (EC/EMC = 3/7 by volume) containing 1.15 M LiPF₆ was purchased from PANAX ETEC (Korea) and used without further purification. *N*-methyl-2-

pyrrolidone (NMP), Trizma[®] base (99.9%), Trizma[®] hydrochloride (99%), 2-(3,4-dihydroxyphenyl)ethylamine hydrochloride (dopamine hydrochloride, 98%), and methanol (CH₃OH) were purchased from Aldrich and used without further purification. Deionized (DI) water (Milli-Q system, Millipore Co., USA, 18.2MΩcm) was used. Microporous polyethylene (PE, ND420, Asahi Kasei E-materials, Japan) separators were used (porosity: 41%, thickness: 20 μm). The Al₂O₃ target was purchased from Taewon Scientific Co., Ltd. (iTASCO, Korea) with 99.99% purity.

Polydopamine (PDA) surface coating

Separators were surface-coated via a simple polydopamine coating method.⁵ Dopamine solution (2 mg mL⁻¹) was prepared using a mixture of Tris buffer solution (PH 8.5, 10 mM) and methanol (CH₃OH/Tris buffer=1/1 in wt.%) as a co-solvent.

Preparation of PDA/Al₂O₃-coated PE separators

Radio-frequency (RF) magnetron sputtering was used to deposit Al₂O₃ on both the bare PE and the PDA-coated PE separators. The target-to-substrate distance was 150 mm and the diameter of the target was 50 mm. The working vacuum pressure of the stainless-steel chamber was 7×10^{-3} torr of argon (99.999%); cooling water was circulated around the target and throughout the chamber to prevent over-heating during deposition. Prior to Al₂O₃ sputtering, the targets were pre-sputtered for 60 min at an RF power of 50 W to remove surface residual contaminants.

Characterization of separators

The surface morphology of various types of separators including bare PE, PDA-coated PE, and PDA/Al₂O₃ was characterized by field-emission scanning electron microscope (FE-SEM; JSM-6390, JEOL, Japan). The thermal stability of the composite separator was observed after it was placed in an oven and heated at 145 °C for 30 min. The thermal shrinkage ratio was calculated using Eq. (1), where A_i and A_f represent the area of the sample before and after the high-temperature storage, respectively:

$$(1) \quad \text{Thermal shrinkage ratio (\%)} = (A_i - A_f) / A_i \times 100$$

The electrolyte uptake amount was determined by following Eq. (2), where W_i and W_f indicate the separator weight before and after electrolyte absorption, respectively:

$$(2) \quad \text{Uptake amount (wt.\%)} = (W_f - W_i) / W_i \times 100$$

The air permeability represented by Gurley number was examined with a Gurley densometer (4110N, Thwing-Albert, USA) by measuring the time necessary for air to pass through a determined volume under a given pressure. The Gurley number was determined according to procedure JIS-P8117 (Japanese Industrial Standards) by measuring the time (s) for 100 cm³ of air to pass through the membrane under a constant air pressure (6.52 psi).

Electrode preparation

A mixture of slurry containing 90 wt.% LiMn₂O₄, 5 wt.% conductive carbon (Super-P), and 5 wt.% PVDF in NMP was employed. The slurry was cast on aluminum foil (15 μm, Sam-A Aluminum, Korea) using a doctor blade. The cast slurry was dried in air at 130 °C for 1 h, and the electrodes were roll-pressed with a gap-control-type roll-pressing machine (CLP-2025, CIS, Korea). The cathode (density: 1.67 g cm⁻³; loading amount: 7.35 mg cm⁻²;

thickness: 44 μm) was punched into a disc shape (radius: 12 mm) and dried at 60 °C for 12 h under vacuum before assembly.

Electrochemical measurements

The ionic conductivity of the separators was evaluated by sandwiching a liquid-electrolyte-soaked separator between two stainless-steel electrodes. To evaluate the effect of the various types of separators on the cell performance, CR2032-type unit half-cells (LiMn₂O₄/Li metal) were assembled in a glove box filled with argon. The unit cells were aged for 12 h and cycled between 3.0 and 4.5 V vs. Li/Li⁺ at C/10 rate (0.088 mA cm⁻²) using a constant-current (CC) mode at for both charging and discharging processes at room temperature. They were then stabilized in three subsequent cycles between 3.0 and 4.5 V vs. Li/Li⁺ at C/5 rate (0.176 mA cm⁻²) at constant-current/constant-voltage (CC/CV) mode for charging and CC mode during discharging processes at room temperature using a charge/discharge cycle tester (PNE Solutions, Korea).

The pulse-power of the unit cells was investigated using hybrid pulse-power characterization (HPPC) test sequence.¹⁸⁻²⁰ The test consists of a 10-s discharge pulse (5C, 4.3mA cm⁻²), a 40-s rest, and a 10-s charge pulse (3.75C, 3.225 mA cm⁻²) were performed at every 10% state-of-charge (SOC) after precycling and high temperature storage. For the latter, the unit cells were stored at 60 °C for 3 days, followed by cooling them down at 25 °C for 10 h.

To evaluate the rate capability, the unit half-cells (LiMn₂O₄/Li metal) were discharged as varying discharge current density from 1 C to 30 C (1 C, 5 C, 10 C, 15 C, 20 C, 25 C, and 30 C), while keeping the charging current density C/2 (0.44 mA cm⁻²). The unit cells were subsequently cycled at a C-rate of C/2 (0.44 mA cm⁻²) for 500 cycles to evaluate the cycle performance. For the rate capability and cycle performance, CC/CV mode and CC mode were used during charging process and discharging process, respectively, between 3.0 and 4.5 V vs. Li/Li⁺ at room temperature.

Results and discussion

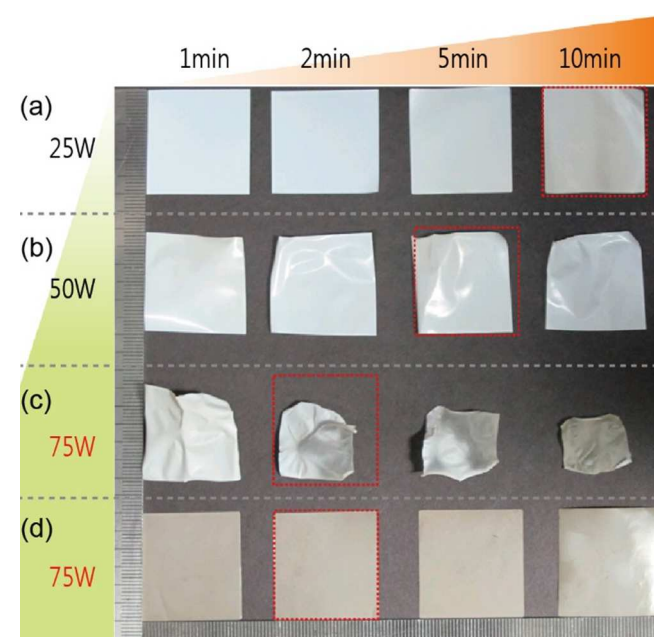


Fig. 1 Digital camera images of (a-c) bare PE separators and (d) polydopamine-coated PE separators exposed to various RF

sputtering powers and times (red-dotted square indicates the original size of separator to be $3\text{ cm} \times 3\text{ cm}$).

As shown in Fig. 1(a-c), the bare PE separators are thermally damaged during high-power RF sputtering at a power over 25W due to the heat accumulated during the process, and the extent of the damage increases with increasing sputtering power. This implies that the RF sputtering process only allows 25W operating power to be used for commercial PE separators. In this study, we introduced sophisticated a mussel-inspired polydopamine (PDA) surface coating upon PE separators, followed by RF sputtering for Al_2O_3 coating.^{5,17,21} PDA-coating can readily adhere to various types of surfaces such as organic, inorganic, and even metallic, and render the surface hydrophilic.^{5,22,23} At least under our experimental condition for PDA and RF sputtering coating processes, due to the nano-scale coating layer thickness, the original pore structures of the bare PE separators were not significantly altered, as shown in Fig. 2.^{5,17}

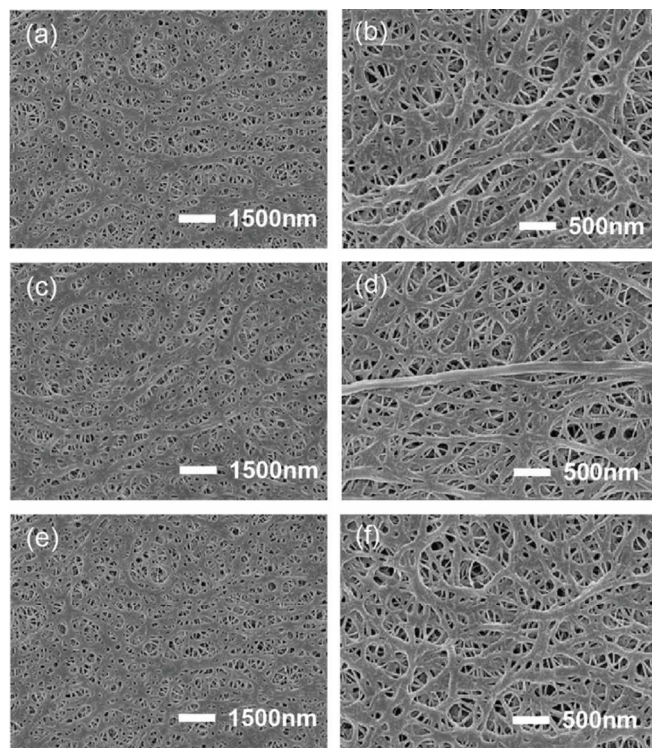


Fig. 2 Scanning electron microscopy (SEM) images of (a, b) bare PE separators, (c, d) PDA-coated PE separators, and (e, f) PDA/ Al_2O_3 -coated PE separators.

Table 1. Properties of separators

System	Thickness (μm)	Gurley number (sec 100 mL^{-1})	Liquid uptake (%)	Ionic conductivity (mS cm^{-1})
Bare PE	20	271	58	0.719
PDA-coated PE	20	295	112	0.759
PDA/ Al_2O_3 -coated PE	20	299	124	0.758

Physical properties of separators like thickness, Gurley number, liquid uptake amount, and ionic conductivity, were investigated and listed in Table 1. As discussed above, nano-scale coating layer thickness did not influence the total thickness of the separators. On the other hand, however, the Gurley number, a good indication of the permeability of a membrane, increased from 271 to 295 and 299 s 100 mL^{-1} after PDA coating and Al_2O_3 sputtering treatment, respectively. As the pores were slightly blocked due to the surface coating, more time was inherently required to pass the air at the same pressure.

Both PDA and Al_2O_3 coating layers are both known to be hydrophilic due to existence of oxygen moiety,^{5,17} and thus both surface coated separators show affinity for polar organic electrolytes as shown in Fig. 3. The released liquid electrolyte droplet (EC/EMC=3/7 containing 1M LiPF_6) immediately spread out over the surface-coated separators, while the hydrophobic bare PE separators maintained the liquid electrolyte droplet in the as-released form over a long period. Consequently, both surface-coated separators turned semi-transparent as liquid filled the pores structures, while bare PE separators remained opaque.

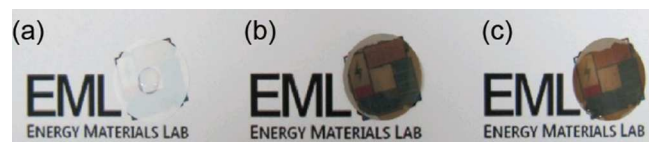


Fig. 3 Digital camera images of separators after a droplet of liquid electrolyte (EC/EMC=3/7 containing 1M LiPF_6) was released upon (a) bare PE separators, (b) PDA-coated PE separators, and (c) PDA/ Al_2O_3 -coated PE separators.

In general, improved wetting ability by surface treatment can increase the ionic conductivity of the bare PE separators, because ionic conductivity mainly depends on the amount of available Li^+ ions associated with liquid electrolyte, under the assumption that the pore structures of membrane are uniform.^{5,21} As listed in Table 1, the liquid electrolyte holding capacities of the PDA-coated PE separators and the PDA/ Al_2O_3 -coated PE separators are 193 % and 214 % more than that of the bare PE separators, respectively. As a result, both the surface-coated PE separators revealed enhanced ionic conductivity compared to the bare PE separators.

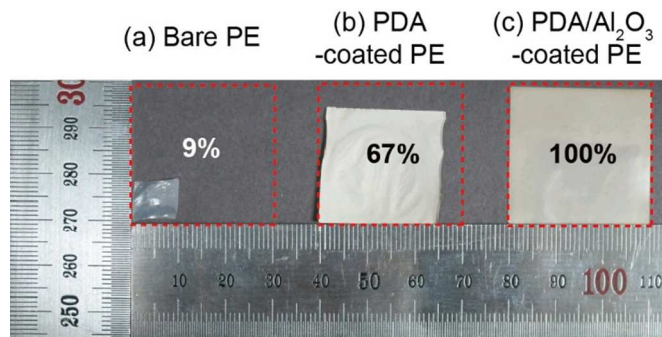


Fig. 4 Digital camera images of (a) bare PE separators, (b) PDA-coated PE separators, and (c) PDA/ Al_2O_3 -coated PE separators after exposure to a temperature of 145°C for 30 min (red-dotted square indicates the original size of separator to be $3\text{ cm} \times 3\text{ cm}$).

For safety issues, dimensional stability of the separators at high temperatures should be the overriding criterion for separator selection. Under abnormal conditions or harsh operating conditions

such as high-power operation, LIBs, in general, generate a large amount of heat, and the separator should not be ruptured and/or

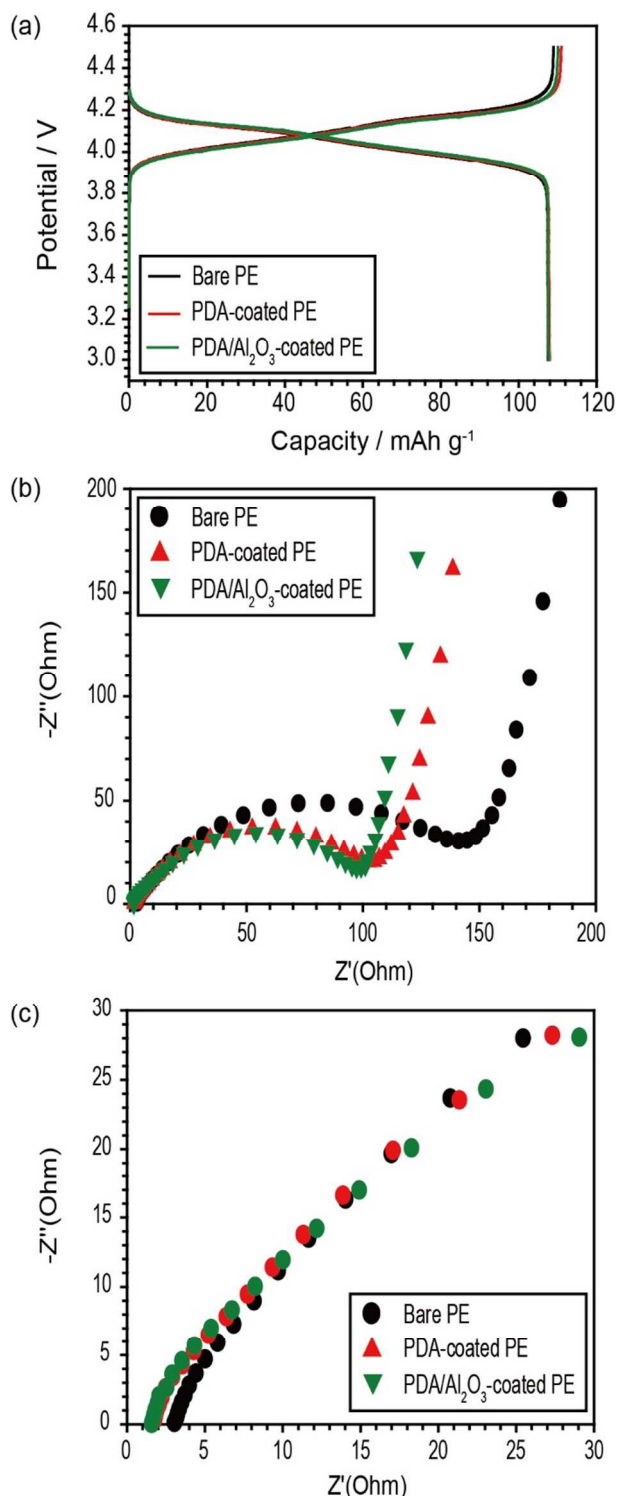


Fig. 5 (a) Voltage profiles of unit cells employing bare PE separators, PDA-coated PE separators, and PDA/Al₂O₃-coated PE separators for the first cycling (CC mode at C/10 between 3.0-4.5 V vs. Li/Li⁺). (b) Nyquist plots for the unit cells after the first cycling, and (c) the same Nyquist plots with a different scale (the unit cells were fully discharged to 3.0 V vs. Li/Li⁺ prior to EIS measurements).

deformed under such conditions to keep the whole LIB system safe. As shown in Fig. 4, various types of separators were exposed to a high temperature, 145 °C for 30 min., and the dimensional changes were monitored for each case. Bare PE separators shrank drastically to only 9 % of their original size after the test. On behalf of thermally stable melanin-like PDA properties, the PDA-coated separators showed improved thermal stability: they maintained 67 % of the original size.^{7,24} Surprisingly, the PDA/Al₂O₃ separators maintained their original dimensions after the same treatment. Considering the fact that we required 40 min. of RF Al₂O₃ sputtering (at 25W) to achieve a similar level of dimensional stability of the Al₂O₃-coated PE separators in our previous study, our new approach, requiring only 2 min. of RF Al₂O₃ sputtering (at 75W), is a more efficient and cost-effective process for mass production.¹⁷

To investigate the effect of surface coating of PE separators on electrochemical properties like rate capability and discharge capacity retention ability, 2032 coin-type unit cells consisting LiMn₂O₄/separator/Li metal were prepared.

As shown in Fig. 5(a), each unit cell employing various types of separators including bare PE, PDA-coated PE, and PDA/Al₂O₃-coated PE, showed almost similar performance during the first cycling operated at a constant current (CC) mode for both charging and discharging processes at C/10 rate between 3.0-4.5 V vs. Li/Li⁺: Bare PE (charge capacity = 108.9 mAh g⁻¹, discharge capacity = 107.6 mAh g⁻¹), PDA-coated PE (charge capacity = 111.0 mAh g⁻¹, discharge capacity = 108.0 mAh g⁻¹), and PDA/Al₂O₃-coated PE (charge capacity = 110.1 mAh g⁻¹, discharge capacity = 107.8 mAh g⁻¹).

After the first cycling, followed by full discharge to 3.0 V vs. Li/Li⁺, electrochemical impedance spectroscopy (EIS) measurements were carried out. In general, the EIS of unit cells is composed of two depressed semicircles and a steep sloping line in the low-frequency regions.^{5,25,26} A small semicircle in the high frequency region (left-handed side) is related to the resistance associated with the solid electrolyte interphase (SEI) layer (R_{SEI}), and a large semicircle (right-handed side) in the medium frequency region corresponds to the resistance of charge-transfer process (R_{ct}), accompanied by migration of the Li⁺ ions at the electrode/electrolyte interface.^{5,27} The x-axis intercept depicts the bulk-resistance (R_b) including the resistances of the electrolyte and electrode.²⁷ As shown in Fig. 5(b), the sum of the resistances ($R_b + R_{SEI} + R_{ct}$) has a higher value for the bare PE than for the two surface-coated cases. As shown in Fig. 5(c), R_b of the bare PE was much larger compared to the others. Keeping in mind that both R_b and R_{ct} are closely related to Li⁺ ion migration, which in turn is closely associated with the wetting ability of separators increasing the degree of electrolyte retention within the separators, it is natural to understand why the PDA-coated PE and PDA/Al₂O₃-coated PE separators have smaller resistances compared to those of bare PE separators.

We also investigated the pulse-power capability of the unit cells using HPPC test sequence.¹⁸⁻²⁰ The discharge pulse-power of unit cells (LiMn₂O₄/Li metal) employing different types of separators were summarized in Fig. 6. After precycling, PDA-coated PE and PDA/Al₂O₃-coated PE separators reveals almost similar discharge pulse-power capability, which are both higher values compared to bare PE, over whole range of SOC from 10 to 90%. After high temperature storage (60 °C, 3 days), the pulse-power of each unit cell was lowered compared to those of precycling case. On the other hand, PDA/Al₂O₃-coated PE separators reveals the best discharge power capability. HPPC results are well consistent with previous ESI results shown discussed above in Fig. 5(b).

To investigate the effect of increased wetting ability of the PDA-coated PE and PDA/Al₂O₃-coated PE separators, we measured

the rate capability and discharge retention ability of the corresponding unit cells.

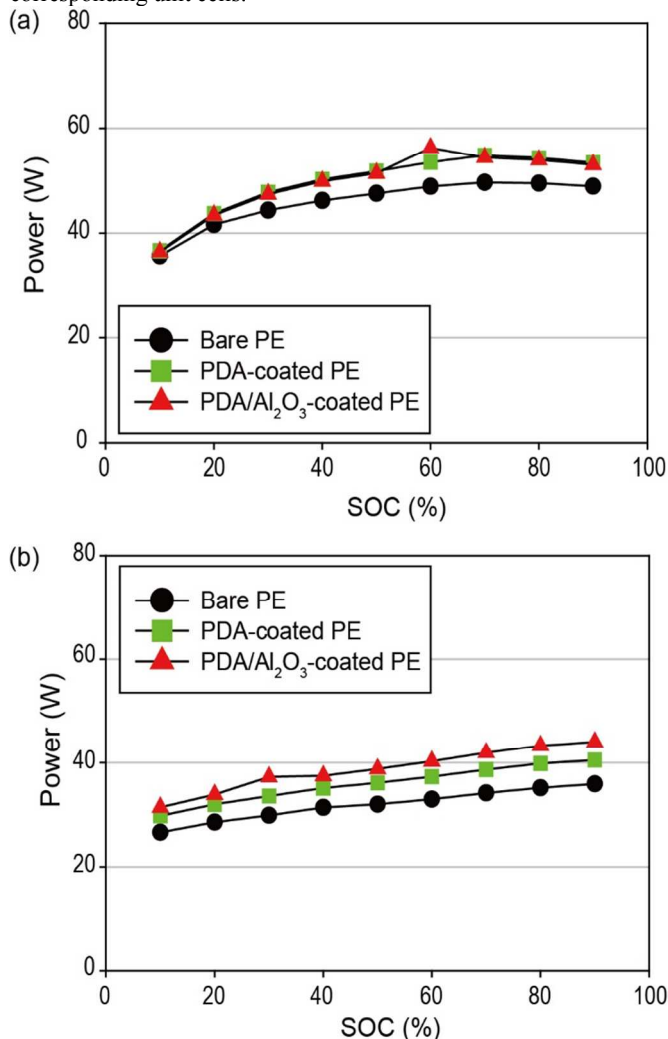


Fig. 6 Pulse-power capability plot for unit cells after (a) precycling and (b) high temperature storage (60 °C, 3 days).

For the rate capability test, the discharge current was varied from 1 C through 30 C (1, 5, 10, 15, 20, 25, and 30 C), keeping the charging current constant ($C/2$, 0.44 mA cm^{-2}). As shown in Fig. 7(a), the PDA-coated PE and PDA/Al₂O₃-coated PE separators showed improved rate capability compared to the bare PE separators. At 25 C rate (at the 30th cycle), the rate capabilities of the PDA-coated PE and PDA/Al₂O₃-coated PE were enhanced by 214 % (58.2 mAh g^{-1}) and 208 % (56.7 mAh g^{-1}), respectively, compared to the bare PE separators (27.2 mAh g^{-1}). The improvement can be elucidated using the improved wetting ability of coated-separators and EIS results discussed in Table 1 and Fig. 5, respectively. The improved wetting ability of the coating layers helps the separators retain greater amounts of liquid electrolytes within their micro-pore structures, which lowers bulk resistance R_b , thus ensuring smooth migration of Li^+ ion between the separators and electrodes due to small interfacial resistance ($R_{\text{SEI}} + R_{\text{ct}}$). When the discharge current was set back to 1 C after 35 cycles, the discharge capacity of the unit cells recovered to the level prior to rate capability test. This indicates that the irreversible material loss during the test is insignificant. From the results, we can infer that the reduced discharge capacity of the unit cells during the rate capability test was due to the kinetic

reason, not to the active material loss caused by electrochemical surface reactions.

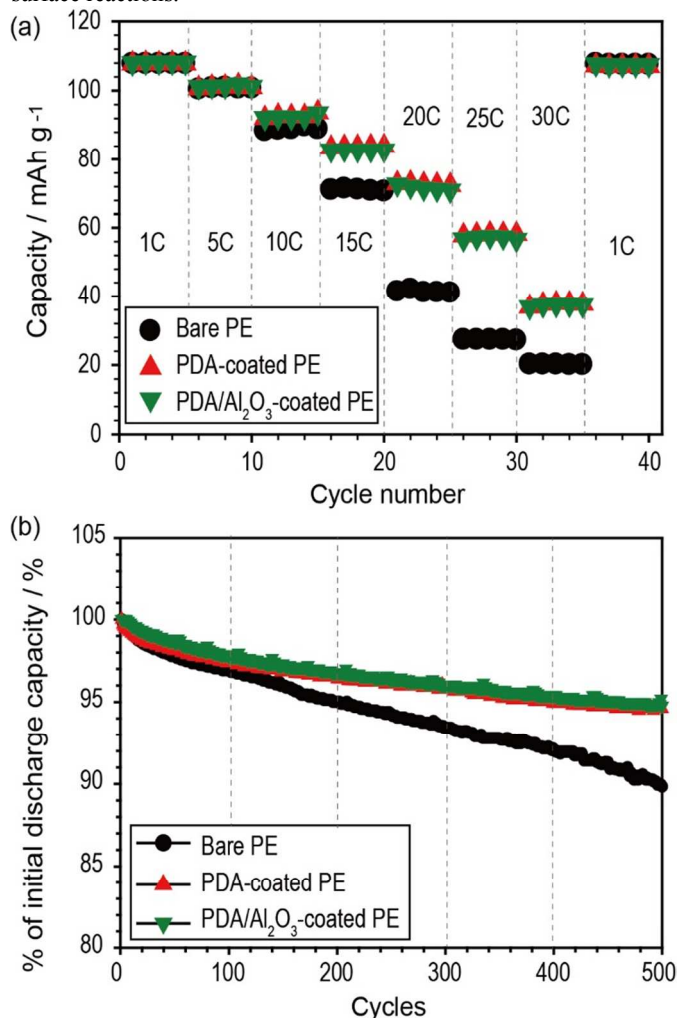


Fig. 7 (a) A comparison of the discharge capacities of unit cells employing different types of separators (bare PE, PDA-coated PE, and PDA/Al₂O₃-coated PE separators) at different discharging current density from 1 C through 30 C, keeping the charging current density at $C/2$. (b) Cycle performances of unit cells operated at $C/2$ for both charging and discharging processes.

To investigate the cycle retention ability of surface-coated separators, the unit cells (LiMn₂O₄/separator/Li metal) employing different types of separators were cycled at $C/2$ rate for both the charging and discharging processes at constant current/constant voltage (CC/CV) mode between 3.0 and 4.5 V vs. Li/Li⁺. As shown in Fig. 7(b), both the surface-coated separators achieved highly improved cycle retention ability compared to the bare PE separators. Bare PE separators retained 89 % (98.6 mAh g^{-1}) of the initial discharge capacity, while PDA-coated and PDA/Al₂O₃-coated PE separators achieved 94.6 % (104.0 mAh g^{-1}) and 94.8 % (103.4 mAh g^{-1}) retention, respectively. Recently, we reported that the homogeneous Li^+ ion flux derived from improved wetting ability of the separators can highly improve the cycle life of Li metal.^{7,28} Here, it is inferred that the improved wetting ability of surface-coated PE separators facilitate the homogeneous Li^+ ion flux over the electrode surfaces resulting in enhanced cycle life.

Fig. 8 shows the potential profiles of the selected cycles during rate capability test demonstrated in Fig. 7(a). Clearly, the

polarization became larger as increasing the current density. On the other hand, the bare PE revealed the larger polarization compared to others. These are well consistent with the larger EIS (Fig. 5(b)) results and the smaller HPPC pulse-power (Fig. 6) results.

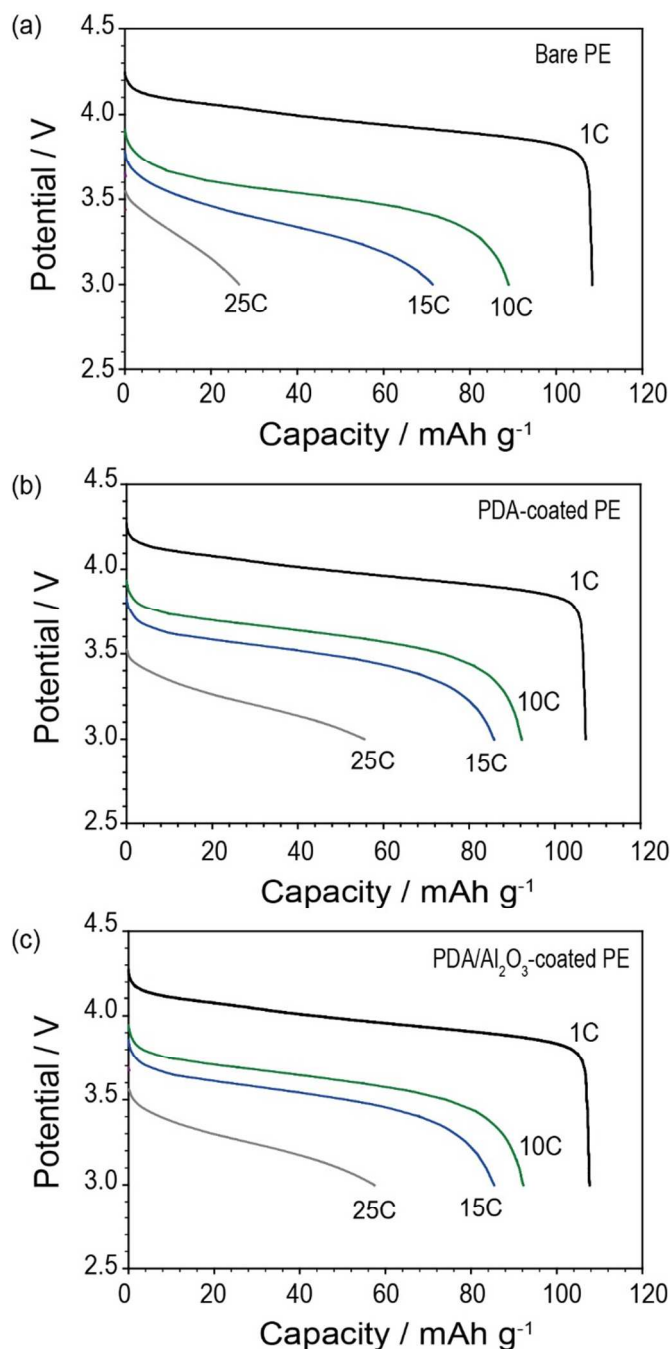


Fig. 8. Potential profiles of the selected cycles (every 5th cycle, 5th, 10th, 15th, 20th, 25th, and 30th) of the unit cells employing (a) bare PE, (b) PDA-coated PE, and (c) PDA/Al₂O₃-coated PE separators during rate capability experiments demonstrated in Fig. 7(a).

Conclusions

With the help of mussel-inspired PDA coating, followed by RF Al₂O₃ sputtering, highly functional PE separators were developed. They demonstrate superior thermal stability at high

temperatures (145 °C), and improved cell performances like rate capability and cycle retention ability. PDA coating enables bare PE separators to sustain high-power Al₂O₃ RF sputtering at remarkably short processing times and enhances the process efficiency. This marks PDA/Al₂O₃-coated PE separators as a promising separator material, targeting large-scale LIB systems ensuring better safety standards and better performance.

Acknowledgements

We acknowledge the financial support by the Ministry of Education, Science and Technology (MEST) and National Research Foundation (NRF) of Korea through the Human Resource Training Project for Regional Innovation (2014066977) and IT R&D program of MOTIE/KEIT (10046314).

Notes and references

^a Department of Chemical and Biological Engineering, Hanbat National University, 125 Dongseodaero, Yuseong-gu, Daejeon 305-719, Republic of Korea.

*Corresponding author. E-mail: yongmin.lee@hanbat.ac.kr; Tel: +82-42-821-1549; Fax: +82-42-821-1692

**Co-corresponding author. E-mail: mhryou@hanbat.ac.kr; Tel: +82-42-821-1534; Fax: +82-42-821-1692

†These authors contributed equally to this work.

1. K. Xu, *Chem. Rev.*, 2004, **104**, 4303-4418.
2. M. Armand and J.-M. Tarascon, *Nature*, 2008, **451**, 652-657.
3. C. Liu, F. Li, L. P. Ma and H. M. Cheng, *Adv. Mater.*, 2010, **22**, E28-E62.
4. N. S. Choi, Z. Chen, S. A. Freunberger, X. Ji, Y. K. Sun, K. Amine, G. Yushin, L. F. Nazar, J. Cho and P. G. Bruce, *Angew. Chem. Int. Ed.*, 2012, **51**, 9994-10024.
5. M.-H. Ryou, Y. M. Lee, J. K. Park and J. W. Choi, *Adv. Mater.*, 2011, **23**, 3066-3070.
6. J. J. Woo, Z. Zhang and K. Amine, *Adv. Energy Mater.*, 2014, **4**, DOI: 10.1002/aenm.201301208.
7. M.-H. Ryou, D. J. Lee, J. N. Lee, Y. M. Lee, J. K. Park and J. W. Choi, *Adv. Energy Mater.*, 2012, **2**, 645-650.
8. Y. Wang, H. Liu, K. Wang, H. Eiji, Y. Wang and H. Zhou, *J. Mater. Chem.*, 2009, **19**, 6789-6795.
9. T.-F. Yi, J. Shu, Y.-R. Zhu, X.-D. Zhu, C.-B. Yue, A.-N. Zhou and R.-S. Zhu, *Electrochim. Acta*, 2009, **54**, 7464-7470.
10. S. S. Zhang, *J. Power Sources*, 2006, **161**, 1385-1391.
11. C. Lin, X. Fan, Y. Xin, F. Cheng, M. O. Lai, H. Zhou and L. Lu, *J. Mater. Chem. A*, 2014, **2**, 9982-9993.
12. M. Baginska, B. J. Blaiszik, R. J. Merriman, N. R. Sottos, J. S. Moore and S. R. White, *Adv. Energy Mater.*, 2012, **2**, 583-590.
13. J. Shi, T. Shen, H. Hu, Y. Xia and Z. Liu, *J. Power Sources*, 2014, **271**, 134-142.
14. Y. Ko, H. Yoo and J. Kim, *RSC Adv.*, 2014, **4**, 19229-19233.
15. H.-S. Jeong and S.-Y. Lee, *J. Power Sources*, 2011, **196**, 6716-6722.
16. J. Song, M.-H. Ryou, B. Son, J.-N. Lee, D. J. Lee, Y. M. Lee, J. W. Choi and J.-K. Park, *Electrochim. Acta*, 2012, **85**, 524-530.
17. T. Lee, W.-K. Kim, Y. Lee, M.-H. Ryou and Y. M. Lee, *Macromol. Res.*, 2014, **22**, 1190-1195.
18. I. Bloom, S. A. Jones, V. S. Battaglia, G. L. Henriksen, J. P. Christophersen, R. B. Wright, C. D. Ho, J. R. Belt and C. G. Motloch, *J. Power Sources*, 2003, **124**, 538-550.
19. H.-W. Lee and Y.-M. Lee, *J. Korean. Electrochem. Soc.*, 2012, **15**, 115-123.
20. PNGV Battery Test Manual, Revision 1, Idaho National Engineering Laboratory, Department of Energy, DOE/ID-10597, May, 1998.

21. S. M. Kang, M.-H. Ryou, J. W. Choi and H. Lee, *Chem. Mater.*, 2012, **24**, 3481-3485.
22. J. H. Waite, *Nat. Mater.*, 2008, **7**, 8-9.
23. H. Lee, S. M. Dellatore, W. M. Miller and P. B. Messersmith, *Science*, 2007, **318**, 426-430.
24. B. Simonovic, V. Vucelic, A. Hadzi-Pavlovic, K. Stepien, T. Wilczok and D. Vucelic, *J. Therm. Anal. Calorim.*, 1990, **36**, 2475-2482.
25. J. Song, H. Lee, Y. Wang and C. Wan, *J. Power Sources*, 2002, **111**, 255-267.
26. J. Li, C. F. Yuan, Z. H. Guo, Z. A. Zhang, Y. Q. Lai and J. Liu, *Electrochim. Acta*, 2012, **59**, 69-74.
27. T.-H. Cho, M. Tanaka, H. Onishi, Y. Kondo, T. Nakamura, H. Yamazaki, S. Tanase and T. Sakai, *J. Power Sources*, 2008, **181**, 155-160.
28. M.-H. Ryou, Y. M. Lee, Y. Lee, M. Winter and P. Bieker, *Adv. Funct. Mater.*, 2015, **25**, 825-825.